Infrared Transmission Spectroscopy of Silver Zeolite A

J. Baumann,† R. Beer, G. Calzaferri,* and B. Waldeck

Institute for Inorganic and Physical Chemistry, University of Berne, CH-3000 Bern 9, Switzerland
(Received: May 6, 1988; In Final Form: September 28, 1988)

A high-vacuum cell attached to the external part of a BOMEM DA3 FTIR instrument is used for in situ transmission experiments on self-supporting zeolite wafers of 15–20 μm thickness, in the spectral range between 20 and 13 800 cm^{-1}. Results on zeolites Linde 4A and Linde 5A and on different Ag^+-exchanged zeolites A in presence of reactants such as H_2O, D_2O, H_2, D_2, CO, and CO_2 demonstrate the high-quality information achieved by this technique. We have been able to obtain clear evidence for the appearance of Evans holes in the H_2O and D_2O stretching vibration on a zeolite A. Furthermore the stretching plus bending bands, the bending plus librational combination bands, and new OH stretching frequencies have been observed. Far-IR spectra of the silver species, the development of new structural OH and OD groups, and the overall transmission have been followed during the reduction of Ag–A zeolites with H_2 and D_2. At different stages of reduction, interaction of CO and CO_2 has been probed and revealed interesting information on structural changes and kinetics under different conditions. The method and data reported open a wide field for detailed investigations on the interaction of metal exchanged zeolites with gaseous reactants.

1. Introduction

Silver zeolites have received wide attention over the past several years following the finding that the brick-red color of thoroughly dehydrated Ag–A zeolite is very sensitive to traces of moisture.[1] It has long been known that Ag^+-containing silicon dioxide is light sensitive[2] and that Ag^+ ions, introduced in the lattice of synthetic zeolite 13X, show luminescence in the visible region when irradiated by UV light.[3] The luminescence behavior depends on the pretreatment of the samples. When studying the hydrogen uptake of Ag–Y zeolite and reoxidation with O_2, Riekert found behavior consistent with the assumption that reduced Ag^0 particles are reoxidized to Ag^+ ions in the lattice while no Ag_2O is formed.[4] In a later study of the redox behavior of transition-metal ions in zeolites, it was observed that the reduction and reoxidation of a silver–Y zeolite with H_2 and O_2 are reversible. In an elegant experiment the authors studied the appearance and disappearance of OH, OD, and CO stretching vibrations on reduction and reoxidation of silver–Y zeolite and upon exposure to CO.[5] Based on ESR studies of the reduction process of silver zeolites, it was reported that hydrogen reduction of dehydrated silver zeolites A and X proceeds via intermediate formation of Ag_6^{n+} ($n < 6$) clusters, located in the cubooctahedral sodalite cages. On further reduction, submicroscopic Ag crystals have been observed, resulting in a conduction electron spin resonance signal.[6] There is an apparent discrepancy between ESR and optical spectroscopic observations concerning the interpretation of the nuclearity of silver species generated by thermal vacuum dehydration in zeolites Y.[7] Furthermore, static susceptibility data from Texter and coworkers[8] provide unequivocal evidence that the silver cluster, giving rise to the 2.7-eV absorption band in "yellow" zeolite A, is not paramagnetic, which means that the assignment of the visible absorption[9] and of the far-IR absorptions[10] to molecular Ag_3^{2+} apparently requires reinvestigation. Molecular orbital calculations lead to the idea that the HOMO region in zeolites consists of many closely spaced, localized states concentrated on the O atoms.[13] Reversible color changes of Ag^+ [1,11] and Cu^+ [12] zeolites observed in dehydration–hydration experiments can be understood as charge-transfer transitions from the HOMO concentrated on the zeolite oxygen atoms to the metal cations. Qualitative and later quantitative photochemical experiments[14-18] have shown that, on illumination of silver zeolites in aqueous dispersions, the silver ions are reduced to Ag^0 and oxygen is evolved. This photoreaction is an interesting candidate for photochemical conversion of solar energy because water splitting, nitrogen fixation, and CO_2 reduction involve the oxidation of water to molecular oxygen. Detailed investigations on the spectral sensitivity on this photooxygen production lead to the surprising result that self-sensitization takes place: the further the reaction proceeds, the more the sensitivity shifts from the initial UV to the visible out into the red spectral range.[16-18] According to the molecular orbital picture,[13] the initial UV photooxygen evolution in Ag zeolites is caused by the oxygen to metal charge transfer. Even in hydrated Ag zeolites there is a sufficient amount of silver ions partly coordinated to zeolite oxygen, so that the concentration of states allowing oxygen to metal transitions at about 370 nm is high enough to permit the initial photooxygen evolution. The zeolite framework is oxidized in each charge transfer until O_2 can evolve. Since the oxidation states of Si(IV) and Al(III) are not changed in aqueous dispersions and since no other reductant is available, the O_2 must originate from water. In the self-sensitization process reduced silver centers are believed to be formed first followed by aggregation to Ag_n^{m+} ($m < n$) which act as chromophores at longer wavelengths. The self-sensitization[16] and its interpretation[13] provide an experimental proof and a theoretical explanation for the observation of Loening and Farnell[2] that silver ions deposited on precipitated silicon dioxide are light sensitive to at least 600

† Present address: Bundesamt für Umweltschutz, Hallwylstrasse 4, CH-3003 Bern, Switzerland.

(1) Rálek, M.; Jírů, P.; Grubner, O.; Beyer, H. *Collect. Czech. Chem. Commun.* **1962**, *27*, 142.
(2) Loening, E. E.; Farnell, G. C. *Photogr. J.* **1952**, *92B*, 187. Burmistrov, F. L. *Photogr. J.* **1936**, 452.
(3) Narita, K. *J. Lumin.* **1971**, *4*, 73.
(4) Riekert, L. *Ber. Bunsen-Ges. Phys. Chem.* **1969**, *73*, 331.
(5) Beyer, H.; Jacobs, P. A.; Uytterhoeven, J. B. *J. Chem. Soc., Faraday Trans. 1* **1976**, *72*, 674.
(6) Hermerschmidt, D.; Haul, R. *Ber. Bunsen-Ges. Phys. Chem.* **1980**, *84*, 902.
(7) Narayana, M.; Kevan, L. *J. Chem. Phys.* **1985**, *83*, 2556. Brown, D. R.; Kevan, L. *J. Phys. Chem.* **1986**, *90*, 1129. Morton, J. R.; Preston, K. F. *J. Magn. Reson.* **1986**, *68*, 121.
(8) Texter, J.; Kellerman, R.; Gonsiorowski, Th. *J. Chem. Phys.* **1986**, *85*, 637. Texter, J.; Kellerman, R.; Gonsiorowski, Th. *J. Phys. Chem.* **1986**, *90*, 2118.
(9) Gellens, L. R.; Mortier, W. J.; Schoonheydt, R. A.; Uytterhoeven, J. B. *J. Phys. Chem.* **1981**, *85*, 2783.
(10) Ozin, G. A.; Baker, M. D.; Godber, J. *J. Phys. Chem.* **1984**, *88*, 4902. Baker, M. D.; Ozin, G. A.; Godber, J. *J. Phys. Chem.* **1985**, *89*, 305.
(11) Kellerman, R.; Texter, J. *J. Chem. Phys.* **1979**, *70*, 1562.
(12) Texter, J.; Strome, D. H.; Herman, R. G.; Klier, K. *J. Phys. Chem.* **1977**, *81*, 333.
(13) Calzaferri, G.; Forss, L. *Helv. Chim. Acta* **1987**, *70*, 465.
(14) Leutwyler, S.; Schumacher, E. *Chimia* **1977**, *31*, 475.
(15) Jacobs, P. A.; Uytterhoeven, J. B.; Beyer, H. K. *J. Chem. Soc., Chem. Commun.* **1977**, 128.
(16) Calzaferri, G.; Hug, S.; Hugentobler, Th.; Sulzberger, B. *J. Photochem.* **1984**, *26*, 109. Calzaferri, G. *Chimia* **1986**, *40*, 74. Calzaferri, G.; Forss, L.; Spahni, W. *Chem. Z.* **1987**, *21*, 161.
(17) Calzaferri, G.; Spahni, W. *J. Photochem.* **1986**, *32*, 151.
(18) Calzaferri, G.; Spahni, W. *Chimia* **1986**, *40*, 435; **1987**, *41*, 200.

0022-3654/89/2093-2292$01.50/0 © 1989 American Chemical Society

TABLE I: Instrumental Configuration of the BOMEM DA3 FTIR Spectrometer for Various Spectral Regions

range, cm^{-1}	source	optical filter	beam splitter	window	detector
20–350	Hg	Si	6-μm Mylar	polyethylene	4K bolometer
325–900	Globar		3-μm Mylar	CsI	Cu:Ge, 4K
700–3900	Globar	Ge	KBr	KBr	MCT
3000–6000	quartz/halogen	Si + sapphire	KBr	KBr	MCT
5000–9300	quartz/halogen	Si	quartz or CaF_2	KBr	InSb
9300–13800	quartz/halogen	Corning CS 7-69	quartz	KBr	InSb

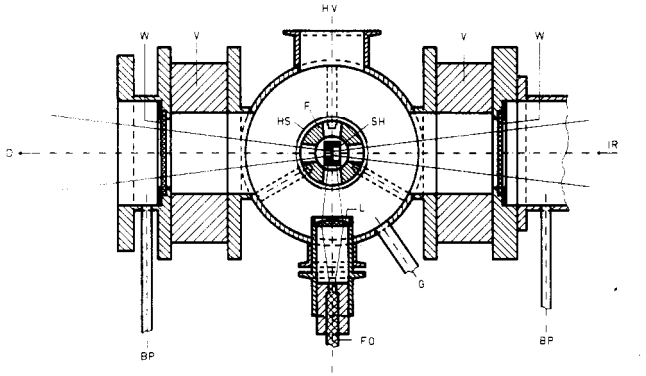

Figure 1. High-vacuum infrared cell, top view. BP, vacuum bypass; CC, cooling connections; CI, ceramic insulation; D, detector; E, electrical feedthrough; F, furnace; FO, fiber optic bundle; G, gas inlet; HS, heat shield; HV, connection to high-vacuum pump; IR, IR beam; L, quartz lens; MC, Macor ceramic; SF, shaft feedthrough; SH, sample holder; V, valve; W, window.

nm. We suspect that in the experiments of these authors oxygen has been produced and that they observed a photoredox reaction of the same kind as reported by us.[16] Their experimental technique, however, was not yet developed far enough to find such evidence.

Given this information, we would like to achieve deeper understanding of the properties of reduced and unreduced Ag zeolites and we are interested in their reactivity toward H_2, H_2O, CO, CO_2, and N_2. Infrared spectroscopy has been extensively used for characterizing clay minerals and zeolites[19] and has found to be a helpful tool for the understanding of adsorbate–zeolite interactions. The sensitivity of Fourier-transform instruments allows us to carry out experiments which have not been possible before. This is the reason for the renewed interest in infrared spectroscopic studies of zeolites in many different laboratories.[20-24] In this paper new results are described, obtained in transmission experiments on self-supporting zeolite wafers of 15–20-μm thickness in the spectral region between 20 and 13 800 cm^{-1}.

2. Experimental Method

A Bomem DA3 FTIR instrument is used in our setup. In order not to be restricted by the dimensions of the instrument's sample compartment, we made use of the possibility to guide the IR beam out of the spectrometer, and we built an external high-vacuum sample cell. The wavelength range investigated extends from 20 to 13 800 cm^{-1}. The various combinations of sources, beam splitters, and detectors used to measure the overall spectra shown in Figure 4 are listed in Table I. Spectral filtering is employed in order to reduce radiation outside the desired band-pass.

A scheme of the high-vacuum infrared cell is shown in Figures 1 and 2. The body is made of stainless steel. The high-vacuum

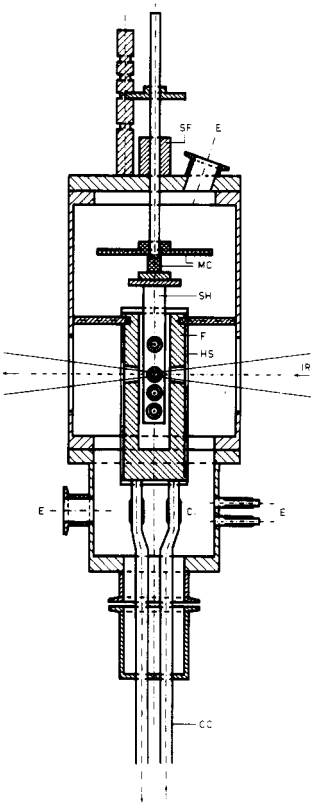

Figure 2. Cross section of the high-vacuum cell. For abbreviations see Figure 1.

pump system consists of a 100 L/s turbomolecular pump, backed by a two-stage mechanical roughing pump. A vacuum of 10^{-6} Torr is thus obtained. The IR beam enters through a suitable window (W) and is focused to a spot of 1–4-mm size at the sample location. Two valves (V) can be closed to protect the windows during heating cycles or gas exposure. A PTI 1000-W Xe lamp in combination with a monochromator is used as illumination source for photochemical studies. The light is guided by a fiber optic bundle (FO) to a quartz lens (L) which seals to the high vacuum and focuses onto the sample. Gases are handled in an independent glass vacuum line and transferred to the sample cell through the gas inlet (G). The sample holder (SH) is fixed to a shaft which can be freely rotated in a way that the sample intersects either the IR beam or the UV/visible light. In addition to this it can be vertically translated. The feedthrough (SF) is located in the removable top cover of the cell and consists of precision graphite seals. Three holes of 4 mm diameter along the vertical axis in the sample holder can insert three sample disks while a fourth hole remains open and is needed for the reference. The sample holder is embedded in a cylindrical furnace (F) to which it has direct contact in its lowermost position. Four holes in the furnace, arranged in a cross-like geometry, allow the IR and visible beams to pass to the sample. To reduce heat loss by radiation, several shields are installed: the furnace itself is surrounded by a thin steel foil (HS) which has only minimal contact to the furnace; two pieces of machinable Macor ceramic (MC) prevent excessive heating of the shaft and its feedthrough, allowing sample temperatures up to 500 °C. The furnace is equipped with an internal channel system connected to two tubings (CC) which are thermally isolated by metal–ceramic (CI) joints and fed

(19) Flaningen, E. M. In *Zeolite Chemistry and Catalysis*; Rabo, J. A., Ed.; ACS Monograph 171; American Chemical Society: Washington, DC, 1976, p 80.
(20) Peuker, C.; Kunath, D. *J. Chem. Soc., Faraday Trans. 1* **1981**, *77*, 2079.
(21) Förster, H.; Frede, W. *Infrared Phys.* **1984**, *24*, 151.
(22) Baker, M. D.; Godber, J.; Ozin, G. A. *J. Am. Chem. Soc.* **1985**, *107*, 3033.
(23) Böse, H.; Förster, H.; Frede, W. *J. Mol. Struct.* **1986**, *143*, 263.
(24) Hoffmann, P.; Knözinger, E. *Surf. Sci.* **1987**, *188*, 181.
(25) Evans, J. C. *Spectrochim. Acta* **1960**, *16*, 994.

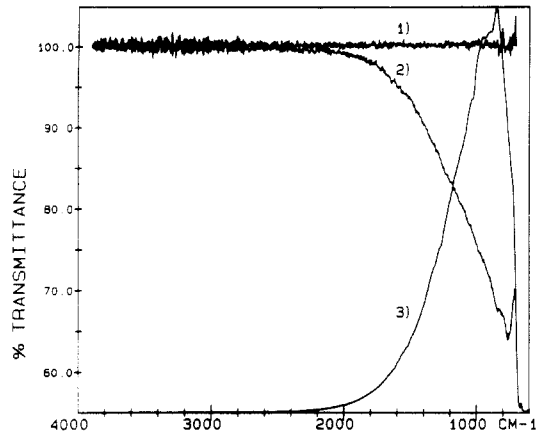

Figure 3. Effect of background radiation with the instrument at room temperature. (1) Lamp spectrum transmitted through an empty sample hole and divided by the reference spectrum taken through the reference hole resulting in a good 100% line. (2) The same as (1) but with the reference spectrum measured with the sample holder completely removed. (3) Thermal background spectrum.

through the bottom of the cell. In addition to heating, it is thus possible to cool the furnace with any suitable coolant. This option is frequently used to shorten the cooling time after heating under vacuum and also makes measurements below room temperature feasible. Temperature control is provided by two Pt-100 resistors, one located at the inside of the furnace, the other one on the sample holder. Since the temperature of the samples is not measured directly, we assume that thermal equilibrium is established within the furnace cavity. This assumption, however, is no longer valid in the low-temperature regime because heating of the sample by the IR beam becomes important as has been shown by Förster et al.[26] at liquid nitrogen temperature. Since the detector housing (D) is not directly connected to the body of the instrument, a bypass (BP) is installed which allows evacuation of the detector housing through the BOMEM vacuum system.

Since the FTIR instrument operates in single-beam mode, a reference spectrum has to be acquired prior to the sample measurements. It is mandatory to measure the reference spectrum under identical instrumental conditions as the sample spectra, including all geometrical constraints at the location of the sample. For this reason a reference hole has been included in the sample holder. Two base lines are shown in Figure 3 to illustrate this point. The holes have been empty for this measurement and the beam has been focused to 1-mm diameter. Curve 1 of Figure 3 is the source spectrum transmitted through an empty sample hole divided by the reference spectrum through the reference hole, resulting in the expected 100% line. In curve 2, however, the reference spectrum has been measured with the sample holder completely removed. Below 2000 cm^{-1} radiation is considerably blocked by the 4-mm aperture of the sample holder although the spot size is 1 mm. The reason is that background radiation originating from aperture and from optical elements of the spectrometer, passing through the interferometer, is more extended at the sample position than the directly transmitted beam from the source. For comparison the background spectrum, obtained by blocking the globar source in the spectrometer, is shown in curve 3. The cutoff at the low-energy side is due to the MCT detector response. The base-line deviation of curve 2 correlates directly with the intensity of the background radiation. This deviation from the ideal 100% line is most pronounced if the spectrometer is operated with a small aperture and thus small throughput as is the case in high-resolution and microsampling applications.

Spectra presented in this paper have been recorded with a 2-cm^{-1} resolution and they are original, unsmoothed data.

Na_{12}–A (Linde 4A) and $Na_{3.6}Ca_{4.2}$–A (Linde 5A) were used as purchased from Union Carbide. For some experiments, Linde 4A has been slurried in a 0.26 M $NaNO_3$ solution for 2 h. $Ag_{11.8}Na_{0.2}$–A was prepared by ion exchange for 2 h with excess of 0.23 M $AgNO_3$ solution. Stoichiometric amounts of 53, 31, 6 mM $AgNO_3$ solutions were used to prepare the partially silver exchanged samples $Ag_{7.5}Na_{4.5}$–A, $Ag_{4.3}Na_{7.7}$–A, and $Ag_{0.9}Na_{11.1}$–A, respectively. After the exchange the samples were washed with bidistilled water and dried under vacuum at room temperature. All operations were performed in the dark. The silver content was analyzed by back-titration of the supernatant solution.

Self-supporting wafers of 15–20-μm thickness and a diameter of about 6 mm are routinely prepared, corresponding to a surface density of 2–2.7 mg/cm^2. Approximately 0.8 mg of the zeolite powder is evenly distributed on a 13 mm diameter steel disk to the required diameter of 6 mm, covered with a second disk, and pressed for 1 min at a pressure of 12–14 kbar. The wafer, although fragile, can still be handled. It is transferred onto one of the holes in the sample holder and clamped with a metal ring. When handling the light-sensitive silver-exchanged zeolites, these operations are performed in a dark room under weak red light. The thickness of the wafers is measured after the experiments with a micrometer to an accuracy of ± 2 μm.

3. Infrared Spectrum of Zeolite A from 20 to 13 800 cm^{-1}

The infrared spectra of zeolites have been a subject of considerable interest during the past years. The range below 1200 cm^{-1} was studied in relation to structural properties of the zeolite framework.[19] Band assignments have been given in terms of structure unspecific SiO_4, AlO_4 vibrations and vibrations of larger entities which are dependent on the actual zeolite structure. Far-infrared studies were performed in addition and the potential of directly probing the exchangeable cations has been demonstrated.[20,27] Furthermore, IR spectroscopy has proven to be a very sensitive technique for measuring adsorbed molecules and their interaction with the zeolite.[28] All these investigations are usually limited to the required frequency range of the bands under study. Since modern FTIR instruments cover an enormous spectral range, we are interested in fully exploiting this capability in order to obtain as much information as possible about the zeolite itself, adsorbate–zeolite interactions, and chemical transformations of adsorbed molecules and the zeolite matrix. The near-IR is included since it is known that Cu–Y zeolite under certain conditions shows low-energy electronic transitions.[29] In Figure 4 we thus present IR transmission spectra of three zeolites A having different cations, from 20 to 13 800 cm^{-1}.

A first inspection of Figure 4 shows that only the four most intense bands show nearly complete obscuration. For undiluted samples this is only possible because very thin wafers of less than 20-μm thickness have been prepared. However, the transmission in the near-IR is found to be very low due to diffuse scattering of the incident radiation. Since we made no attempt to completely dehydrate our samples, adsorbed water was always present. For this reason we first discuss the absorption of water.

The water molecule in the gas phase has three IR-active vibrations: the bending mode ν_2 and two stretching modes, symmetric ν_1 and asymmetric ν_3.[30] In going to the condensed phase several complications arise:[31] Due to hydrogen bonding the stretching frequencies are lowered, and the bending frequency shifts to a higher value while the bands broaden. The broadening reflects first the inhomogeneity of hydrogen bonding and second the intermolecular vibrational couplings. In analogy to ice spectra there are additional bands due to the association of the molecules. In the range of about 300–900 cm^{-1} a broad band appears with

(26) Förster, H.; Meyn, V.; Schuldt, M. *Rev. Sci. Instrum.* **1978**, *49*, 74.

(27) Baker, M. D.; Ozin, G. A.; Godber, J. *Catal. Rev.-Sci. Eng.* **1985**, *27*, 591 and references cited therein.

(28) See e.g.: Ward, J. W. In *Zeolite Chemistry and Catalysis*; Rabo, J. A., Ed.; ACS Monograph 171; American Chemical Society: Washington, DC, 1976; p 118.

(29) Jacobs, P. A.; de Wilde, W.; Schoonheydt, R. A.; Uytterhoeven, J. B.; Beyer, H. *J. Chem. Soc., Faraday Trans. 1* **1976**, *72*, 1221.

(30) Smith, Jr., D. F.; Overend, J. *Spectrochim. Acta* **1972**, *28A*, 471.

(31) Eisenberg, D.; Kauzmann, W. *The Structure and Properties of Water*, Oxford University Press: London, 1969.

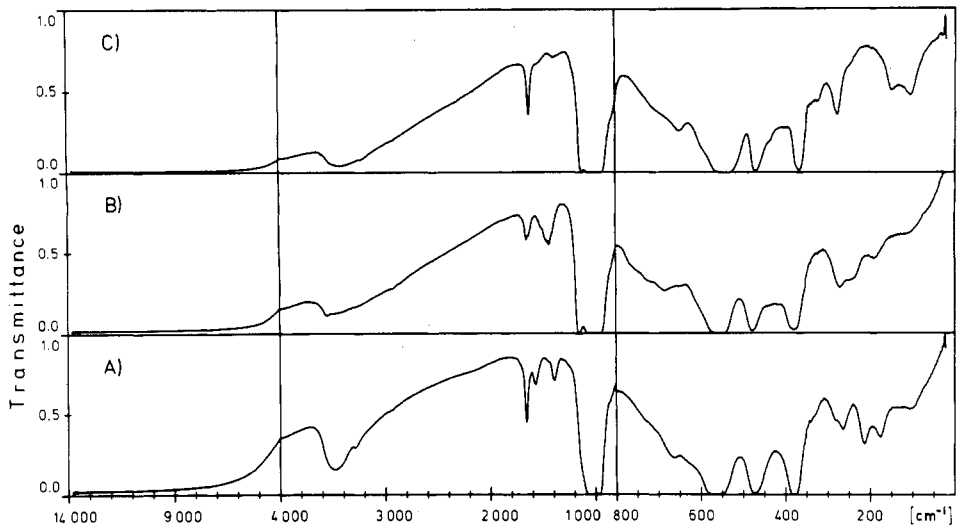

Figure 4. Transmission spectra of self-supporting wafers of (A) Na_{12}–A (Linde 4A), (B) $Na_{3.6}Ca_{4.2}$–A (Linde 5A), (C) $Ag_{11.8}Na_{0.2}$–A; evacuated to 2×10^{-6} Torr at 25 °C.

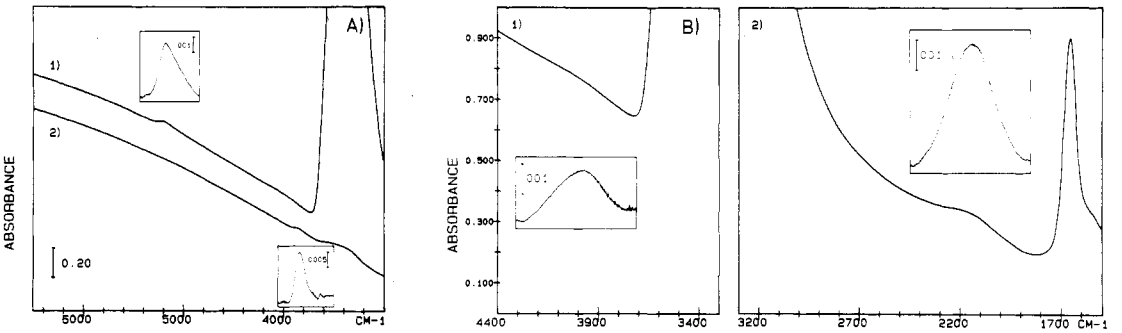

Figure 5. (A) (0110) combination band of (1) H_2O and (2) D_2O adsorbed on sodium zeolite A (Linde 4A). The samples were pretreated at 25 °C by evacuation overnight. The spectra are taken after addition of 20 Torr of H_2O and 14 Torr of D_2O, respectively. (B) (1) (0011) combination band and (2) (0101) combination band of H_2O adsorbed on sodium zeolite A. Sample 1 had a thickness of 18 μm and the spectrum was taken after addition of 20 Torr of H_2O. Sample 2 had a thickness of 21 μm and was evacuated to about 10^{-2} Torr, and the spectrum was taken after half an hour.

a frequency ratio for deuterium substitution of 1.35. This band is assigned as a hindered rotation or libration mode ν_L. There is some discrepancy in the literature about the number and the position of maxima. An absorption at about 200 cm^{-1} with an isotope effect of 1.03 is interpreted as hindered translation ν_T or as the stretching vibration of a hydrogen bond.[32] A summary of the combination and overtone absorption bands and their intensities in liquid H_2O, D_2O and HDO is given by Bayly et al.[33a] They assign the bands as combinations of ν_1, ν_2, ν_3, and ν_L [$(\upsilon_1\upsilon_2\upsilon_3\upsilon_L)$]. In the range between 1000 and 6000 cm^{-1} there are besides the three fundamental modes a combination of ν_2 and ν_3 (0110) and three combination modes which include the libration mode ν_L [(0101), (0011), and (0111)]. In the zeolite spectra a broad OH stretching band appears around 3500 cm^{-1} and the sharper bending mode around 1650 cm^{-1}, see Figures 4 and 8. It is very interesting that we have been able to measure the combination mode of the stretching and bending vibration (0110) for H_2O and D_2O adsorbed on zeolite A which are located in the region of the diffuse scattering (Figure 5A). The combination of the bending mode ν_2 and the libration mode ν_L (0101) appears at 2137 cm^{-1} (liquid water 2125 cm^{-1}) and the combination of the stretching mode ν_3 and the libration mode ν_L (0011) at 3990 cm^{-1} (liquid water 3920 cm^{-1}) (Figure 5B). The (0111) vibration (intensity given by Bayly: $\epsilon = 0.095$ cm^{-1} mol^{-1} at 5595 cm^{-1}, which is about 10 times smaller than the ϵ value of the (0110) band) could not be observed in our experiments. It is, however, observed in diffuse reflectance experiments.[33b] Other details of the water absorptions are given in the next section.

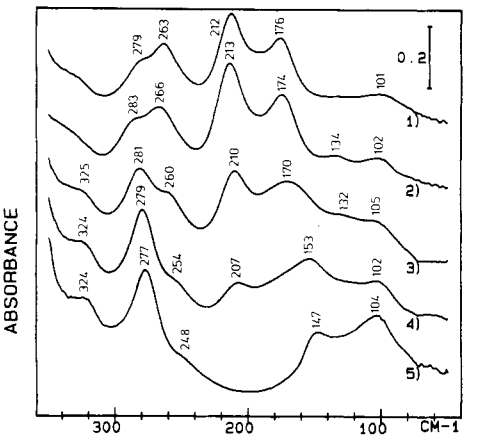

Figure 6. Far-IR spectra of zeolite Linde 4A at different degrees of exchange with silver, evacuated to 2×10^{-6} Torr at 25 °C; the spectra are numerically scaled to a sample thickness of 20 μm. (1) Na_{12}–A (Linde 4A), (2) $Ag_{0.9}Na_{11.1}$–A, (3) $Ag_{4.3}Na_{7.7}$–A, (4) $Ag_{7.5}Na_{4.5}$–A, (5) $Ag_{11.8}Na_{0.2}$–A.

The window between 1200 and 1600 cm^{-1} contains weak bands which are most intense if silver is absent. These bands belong to chemisorbed CO_2 species in the zeolite.[34,35] This assignment is substantiated by the observation that the above-mentioned bands irreversibly increase in intensity on CO_2 adsorption and disappear only on thermal treatment above 200 °C. The strong bands between 300 and 1200 cm^{-1} are relatively insensitive to the cations.

(32) Walrafen, G. E. *J. Chem. Phys.* **1964**, *40*, 3249.
(33) (a) Bayly, J. G.; Kartha, V. B.; Stevens, W. H. *Infrared Phys.* **1963**, *3*, 211. (b) Shen, J. H.; Zettlemoyer, A. C.; Klier, K. *J. Phys. Chem.* **1980**, *84*, 1453.
(34) Schumann, M. Ph.D. Thesis, University of Hamburg, 1986.
(35) Baumann, J.; Beer, R.; Calzaferri, G. *Chimia* **1988**, *42*, 100.

In accordance with ref 19 we assign them to framework vibrations. The far-IR part is of some interest because vibrations of the cations can be probed directly.

Figure 6 demonstrates how the far-IR spectrum develops on going from completely Na^+ exchanged to fully Ag^+ exchanged zeolite A. The spectrum of the fully silver exchanged sample is similar to the one reported by Ozin et al.[36] Literature data are also available for the Na^+ form,[27] although only in the dehydrated state. Despite the different level of hydration of our sample and the one reported in ref 27 the spectra are similar. In going from Na_{12}–A to Ag_{12}–A the two bands at 212 and 176 cm^{-1} are gradually replaced by the doublet at 147 and 104 cm^{-1}. It is thus clear that these bands are attributable to vibrational modes that involve mainly motions of the cations against the quasi-rigid zeolite framework, as has originally been proposed by Brodskii.[37] The individual frequencies have been related to cations at different sites.[27] At low silver content (curves 2 and 3) a weak band at 134 cm^{-1} is observed almost absent in the parent material Linde 4A; however, if Linde 4A zeolite is first slurried in a 0.26 M $NaNO_3$ solution and then washed with water, this band also appears with equal intensity as in curve 2. Its origin is not yet evident. In contrast to the low-frequency bands, the band system between 250 and 350 cm^{-1} has not received much attention. It can be seen that within the doublet 263/279 cm^{-1} of Na_{12}–A the 263-cm^{-1} band gradually disappears on silver exchange while the 279-cm^{-1} band remains basically unchanged and a shoulder is enhanced at 325 cm^{-1}. The doublet character of this band has not been reported in the past. The whole band was attributed to a framework vibrational mode and a recent lattice vibrational calculation characterizes it as a pore opening mode of the double four-ring.[38] In light of the spectra in Figure 6, however, this assignment has to be reconsidered. We first checked whether hindered translation of residual water could be responsible for one band of the doublet. No change in the spectra 1 and 2 of Figure 6 was detected when the samples were saturated with D_2O prior to evacuation. This is not in accordance with the isotopic ratio of 1.03 for this band. In case residual water not being responsible for the band the following explanations can be put forward: first, the 263-cm^{-1} band of Na_{12}–A could be attributed to a new, hitherto unrecognized Na^+ vibration. This Na^+ would have to occupy the most strongly coordinating site and be removed first on Ag^+ exchange. The crystal structure of dehydrated $Ag_{7.6}Na_{4.4}$–A[39] indeed reveals that silver ions prefer the sites in oxygen six-rings expected to be energetically most favorable for both Ag^+ and Na^+ because trigonal coordination to three oxygen atoms at small distance is possible. Second, if an interionic contribution to the 263/279-cm^{-1} doublet is disregarded, one can postulate a cation-dependent splitting of the framework mode into two bands. It is, however, not straightforward to rationalize why the splitting should be so different for Na^+ or Ag^+, since the cations occupy basically the same sites in Na_{12}–A[40,41] and Ag_{12}–A,[42] irrespective of their degree of hydration. The question has to be left open until systematic investigations of Linde 4A zeolites with various other cations than presented here are available. Although this is the case for Li^+, K^+, Tl^+, NH_4^+, Rb^+, and Cs^+,[43] the quality of these spectra is not sufficient to allow a detailed comparison.

4. Reduction of Silver Zeolite A by H_2 and D_2

Silver zeolite reduction can be summarized by

$$[(Ag^+)_n, mH_2O]Z + (r/2)H_2 \rightarrow [Ag_n^{(n-r)+}, rH^+, mH_2O]Z$$

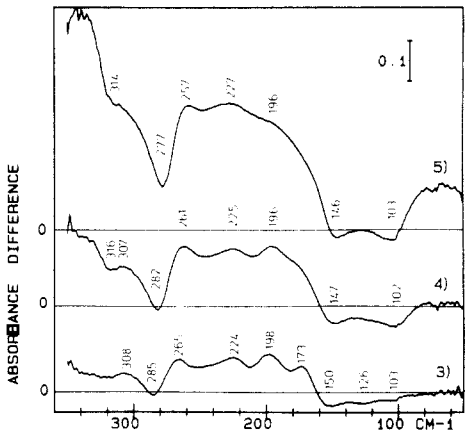

Figure 7. Far-IR difference spectra after 50-min reduction with 200 Torr of H_2 at 100 °C. The curves directly show the spectral changes upon reduction. Prior to reduction the samples were evacuated for 3 h at 25 °C and 2×10^{-6} Torr. The spectra are numerically scaled to a sample thickness of 20 μm. (3) $Ag_{4.3}Na_{7.7}$–A, (4) $Ag_{7.5}Na_{4.5}$–A, (5) $Ag_{11.8}$-$Na_{0.2}$–A.

where Z denotes the zeolite framework. In addition to the formation of partially reduced silver clusters whose nuclearity is still a matter of debate and seems to be sensitive to the actual conditions of the preparation and to the zeolite framework, protons are incorporated into the zeolite to balance the negative charge of the framework. These protons are to some extent associated with framework oxygen atoms and show sharp hydroxyl stretching bands at the high-frequency side of the broad water absorption. These structural OH groups have been subject of many IR spectroscopic investigations on zeolites X, Y, mordenite, and others;[44] to our knowledge, however, no report of similar observations has been given for zeolite A, probably because of the weakness of these bands. Since residual water is always present in our experiments, reduction by D_2 leads to isotopic exchange of H_2O into HOD and D_2O. There are thus several spectral signatures that can be followed during reduction: the far-IR for direct probing of the silver species; the development of structural OH or OD groups; the water bands; the overall transmission which decreases with reduction of the Ag^+ ions; vibrations of a label such as adsorbed CO and CO_2.

Far-Infrared Results. Let us first discuss the changes of the far-IR absorption spectrum when partially dehydrated silver zeolites of various silver content are reduced by 200 Torr of H_2 at 100 °C for 50 min. After reduction the colors of the initially white samples are brown to black, depending on the degree of silver exchange. The difference spectra shown in Figure 7 have been obtained by subtracting the spectra reported in Figure 6 from those measured after reduction. They reveal the disappearance and enhancement of bands found in the unreduced state and the formation of new bands. The whole pattern develops simultaneously as has been observed by a sequence of spectra taken every 5 min during reduction. In the sample of low silver content (sample 3) at least half of the changes after 50 min reduction are already present after 5 min, while in the high-silver-loaded sample 5 the development of the difference spectrum occurs more steadily. In addition to new spectral features, a broad absorption or reflection is built up, increasing in strength toward higher frequencies and continuing into the mid-IR. This broad band loss, referred to as background contribution, increases parallel with the silver content and is most pronounced in the fully silver exchanged zeolite. Due to this background, the shape of which can only be guessed, it is not possible to unambiguously interpret the difference spectra in terms of absorption losses or gains. However, negative peaks certainly correspond to a decrease of bands which is the case for features around 150 and 103 cm^{-1} in all samples as well

(36) Baker, M. D.; Godber, J.; Ozin, G. A. *J. Phys. Chem.* **1985**, *89*, 2299.
(37) Brodskii, I. A.; Zhdanov, S. P.; Stanevich, A. E. *Opt. Spectrosk. (Engl. Transl.)* **1971**, *30*, 58; *Sov. Phys. Solid State* **1974**, *15*, 1771. Brodskii, I. A.; Zhdanov, S. P. *Proc. 5th Int. Zeolites Conf.* **1980**, 234–241.
(38) No, K. T.; Bae, D. H.; Jhon, M. S. *J. Phys. Chem.* **1986**, *90*, 1772.
(39) Kim, Y.; Seff, K. *J. Phys. Chem.* **1987**, *91*, 671.
(40) Gramlich, V.; Meier, W. M. *Z. Kristallogr.* **1971**, *133*, 134.
(41) Yanagida, R. Y.; Amaro, A. A.; Seff, K. *J. Phys. Chem.* **1973**, *77*, 805. Subramanian, V.; Seff, K. *J. Phys. Chem.* **1977**, *81*, 2249.
(42) Kim, Y.; Seff, K. *J. Phys. Chem.* **1978**, *82*, 1071.
(43) Maxwell, I. E.; Baks, A. *Adv. Chem. Ser.* **1973**, *121*, 87.
(44) Angell, C. L.; Schaffer, P. C. *J. Phys. Chem.* **1965**, *69*, 3463. Jacobs, P. A.; Uytterhoeven, J. B. *J. Chem. Soc., Faraday Trans. 1* **1973**, *69*, 359, 373. Dombrowski, D.; Hoffmann, J.; Fruwert, J.; Stock, T. *J. Chem. Soc., Faraday Trans. 1* **1985**, *81*, 2257.

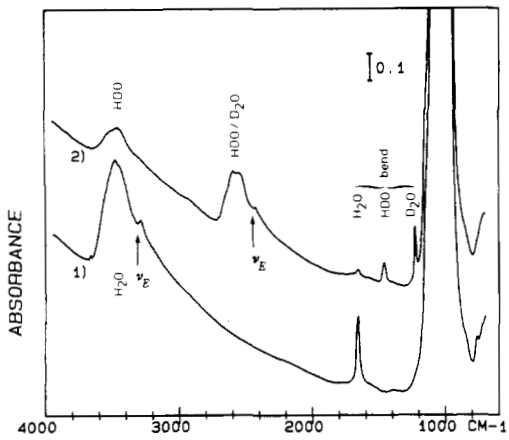

Figure 8. Adsorption of H_2O and D_2O on $Ag_{4.3}Na_{7.7}$–A: (1) evacuation for 3 h at 25 °C; (2) as in (1), then loaded with 15 Torr of D_2O and evacuated for 35 min. ν_E stands for the abbreviation for Evans hole (for explanation see text).

as 285 and 282 cm^{-1} in samples 3 and 4, respectively. The former two bands have been attributed in section 3 to Ag^+ vibrations against the zeolite framework; these bands can be expected to disappear as the silver ions are reduced. The doublet around 280/260 cm^{-1} has already been discussed in section 3 and was assigned to a framework mode or possibly a high-frequency Na^+ interionic vibration. Figure 7 illustrates that on reduction the higher frequency component of the doublet decreases in intensity in favor of the lower frequency band. Although the depression at 277 cm^{-1} in curve 5 does not extend to negative values, we consider this feature, in analogy to 3 and 4, as an absorption loss, the whole pattern being positively offset by the background contribution. Reduction of the zeolite does therefore influence the framework, either by blocking certain vibrational degrees of freedom when silver particles large enough are formed or by influencing the lattice. Three new bands, not present in the unreduced state, are found in all three samples at essentially the same frequencies, most clearly seen in sample 3 (224, 198, 173 cm^{-1}). Whether the positive protrusion at 65 cm^{-1} in sample 5 is really a new band depends on the actual offset by the background contribution. When the reduced samples after exposition of 20 Torr of water vapor at 25 °C are reevacuated the background contribution increases enormously in sample 5 but negligibly in sample 3. Therefore, it can be concluded that this background contribution to the absorption spectrum directly depends on the silver content, increases on reduction, and is enhanced by the presence of water. The three above-mentioned new structured bands can be attributed to silver clusters formed in the course of the reduction.

Water and Hydroxyl Bands. During the reduction with H_2 or D_2 protons or deuterons are produced and remain in the zeolite to balance the negative charge of the lattice. Note, however, that H^+ is found to partially diffuse into the solution if the reduction is carried out in an aqueous dispersion.[16] The protons within the zeolite are associated with oxygen atoms and can be detected by new sharp hydroxyl stretching vibrations in the infrared spectrum. Before analyzing these new bands we consider the fundamental vibrational bands of three isotopic molecules in more detail.

The broadening of the water vibrational absorption bands in condensed phase due to intermolecular vibrational coupling can be suppressed by diluting very small amounts of one water isotope in the other isotope.[31] Assuming that D_2O is the minor species, HDO is instantly formed in the H_2O solvent. At low concentration the HDO molecules are isolated from each other and no coupling of the OD stretching vibration occurs with neighboring H_2O molecules nor intramolecularly with the OH vibration. The thus observed OD absorption bandwidth is related to the heterogeneity of the local structure only. HDO possesses a low-frequency stretching vibration which corresponds to a basically isolated OD stretching vibration and whose frequency lies between the symmetric ν_1 and the asymmetric mode ν_3 of D_2O and a high-frequency component for the OH stretching. In higher concentrations of isotopic solutions or in the isotopically pure phase, intermolecular vibrational coupling occurs which further broadens the stretching bands. In contrast the bending modes ν_2 remain comparatively narrow.

TABLE II: (A) ν_2 Frequencies (cm^{-1}) of Three Isotopic Water Molecules Adsorbed on Silver A Zeolites.[a] (B) Frequencies of the (0110) Combination Band (cm^{-1}) of H_2O and D_2O Adsorbed on Some A Zeolites

A

	H_2O	HDO	D_2O	$\nu(H_2O)/\nu(HDO)$	$\nu(H_2O)/\nu(D_2O)$
gas phase[30]	1594.59	1402.20	1178.33	1.137	1.353
liquid[31]	1645	1447	1215	1.137	1.354
Na_{12}–A[b]	1663	1462	1223	1.137	1.360
$Ag_{0.9}Na_{11.1}$–A	1664	1466	1225	1.135	1.358
$Ag_{4.3}Na_{7.7}$–A	1657	1459	1221	1.136	1.357
$Ag_{7.5}Na_{4.5}$–A	1651	1452	1218	1.137	1.356
$Ag_{11.8}Na_{0.2}$–A	1637	1440	1210	1.137	1.353

B

	H_2O	D_2O	$\nu(H_2O)/\nu(D_2O)$
Na_{12}–A (Linde 4A)	5185	3835	1.352
$Na_{3.6}Ca_{4.2}$–A (Linde 5A)	5184	3834	1.352
$Ag_{11.8}Na_{0.2}$–A	5165	3820	1.352

[a] Samples were evacuated at 25 °C. [b] Washed in a 0.26 M $NaNO_3$ solution.

In Figure 8 the absorption spectra of $Ag_{4.3}Na_{7.7}$–A as a typical example are shown with H_2O (curve 1) and after partial isotopic exchange with D_2O (curve 2). We first focus on the ν_2 bands of H_2O, HDO, and D_2O adsorbed on different silver zeolites A (Table IIA). H to D exchange was performed by repeated cycles of D_2O adsorption and evacuation at room temperature. D_2O used for deuteration was slightly polluted with H_2O so that always HDO and small amounts of H_2O are found. The ν_2 frequency is found to be cation dependent, decreasing with the Na^+ by Ag^+ exchange. The most pronounced shift occurs on exchange of the last four Na^+ by Ag^+. The frequency ratios of the three different isotopic water molecules are constant within experimental error for all samples studied and are equal to the ratio found in the gas and in the liquid phase. The half-width and intensity of the ν_2 band decrease on evacuation. The water stretching band of fully hydrated zeolites A is very broad and intense. On evacuation its bandwidth decreases in Na^+-rich zeolites A while remaining basically constant in the fully Ag^+ exchanged sample. There is some indication of a fine structure in the absorption maximum which is not analyzed in detail here. Note that in the deuterated sample the broad band around 2550 cm^{-1} contains contributions from both D_2O and HDO. When evacuated, some of the water desorbs and two new distinct features evolve in the stretching region of H_2O and D_2O: a sharp peak at the low-frequency edge and sharp weak bands at the high-frequency side of the stretching absorption. Their appearance seems to depend on the existence of relatively isolated water molecules since they are not existent or substantially broadened in the fully hydrated situation where strong intermolecular interactions are expected. The high-frequency components are assigned to structural OH and OD vibrations respectively and will be described in the next paragraph. The low-frequency feature around 3300–3250 and 2441–2411 cm^{-1}, respectively, can be analyzed in terms of Fermi resonance between the first overtone of ν_2 and the stretching mode of the same symmetry. It was shown[45] that this Fermi resonance can be observed in the dihydrates of several tetrachlorocuprates(II). The authors found a similar feature as discussed here and interpreted their results in terms of so-called Evans holes.[25] An Evans hole is a decrease in absorbance which occurs if a weak, sharp band, in our case the $2\nu_2$ overtone, overlaps a broad band

(45) Othen, D. A.; Knop, O.; Falk, M. *Can. J. Chem.* **1975**, *53*, 3837. Thomas, G. H.; Falk, M.; Knop, O. *Can. J. Chem.* **1974**, *52*, 1029.

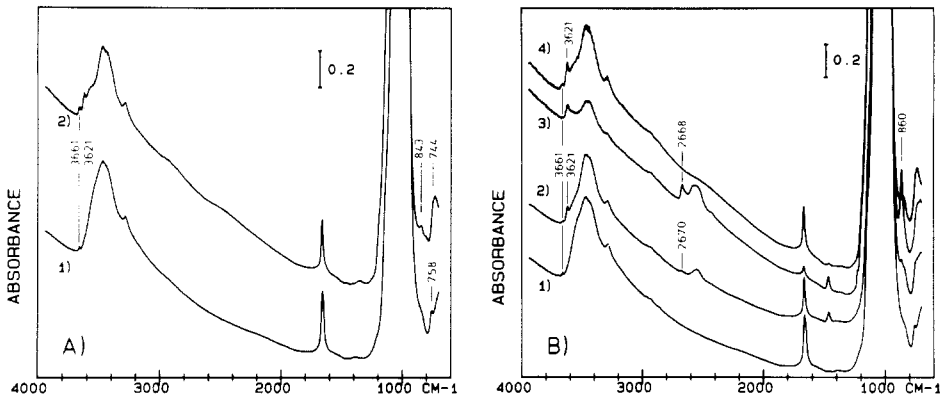

Figure 9. (A) Reduction of $Ag_{4.3}Na_{7.7}$–A with H_2: (1) evacuation for 2 h at 25 °C; (2) 13-min reduction with 200 Torr of H_2 at 100 °C, cooling to 25 °C within 5 min, followed by dynamic evacuation for 15 min. (B) Reduction of $Ag_{4.3}Na_{7.7}$–A with D_2: (1) evacuation for 2 h at 25 °C; (2) 2.5-h reduction of (1) with 200 Torr of D_2 at 25 °C followed by evacuation; (3) 20-min reduction of (2) with 200 Torr of D_2 at 100 °C followed by evacuation and then cooling to 25 °C within 20 min.; (4) addition of 23 Torr of H_2O to (3) followed by evacuation.

TABLE III: Fermi Resonance in H_2O and D_2O Adsorbed on Silver A Zeolites[a]

	Evans hole ν_E		ν_E/ν_2	
	H_2O	D_2O	H_2O	D_2O
Na_{12}–A[b]	3314	2441	1.993	1.996
$Ag_{0.9}Na_{11.1}$–A	3314	2443	1.992	1.994
$Ag_{4.3}Na_{7.7}$–A	3307	2442	1.996	2.000
$Ag_{11.8}Na_{0.2}$–A	3246 ± 10 (sh)	2411	1.983 ± 0.006	1.993

[a] Frequencies are in cm^{-1}. [b] Washed in a 0.26 M $NaNO_3$ solution.

which is due to a vibration of the same symmetry. In this case, Fermi resonance is manifested by the appearance of an absorption hole at the frequency of the overtone and redistribution of the intensity to both sides of this hole.

In Table III we list the frequency of this Evans hole, which is marked by an arrow in Figure 8, and correlate it to the bending vibration ν_2. It is seen that in all cases the hole occurs at nearly exactly the $2\nu_2$ frequency in both H_2O and D_2O loaded zeolites, while it is neither observed in the OH stretching band of diluted HDO in D_2O (Figure 8, curve 2) nor in the OD stretching band of diluted HDO in H_2O. This is indeed expected if Fermi resonance is responsible for the hole since there is no overlap of the HDO bending overtone with either of its two stretching bands. Evidence for an Evans hole is also found in the spectra of slightly hydrated Na^+ and Li^+ zeolites X reported by Bertsch et al.[46] These authors, however, did not interpret the fine structure of their spectra at 3200–3300 cm^{-1}. We have observed a hole in Na^+–X and –Y zeolite; it is located at 1.991 and resp. 1.995 times the bending frequency. It should be noted that this hole is not present in liquid water nor in the fully hydrated zeolites but was probably observed in ice.[31] The sample $Ag_{7.5}Na_{4.5}$–A showed not one hole but two slight depressions, one in the range of the hole in $Ag_{4.3}Na_{7.7}$–A, the other one close to the hole in $Ag_{11.8}Na_{0.2}$–A. As the frequencies could not be determined accurately, this sample has been omitted in the table. The doublet of holes in this sample has its counterpart in a doublet of structural hydroxyl groups discussed below.

The weak sharp bands at the high-frequency side of the broad OH or OD stretching band are of particular interest for our investigations. They have been known for a long time in zeolites X and Y[44] where assignments to structural hydroxyl groups have been proposed. However, to our knowledge no comparable account of sharp hydroxyl bands in zeolite A has been given. They are compiled in Table IV.

A pronounced hydroxyl band at 3713 cm^{-1} (Figure 12A, curve 1, lower trace) is found after washing the zeolite in 0.26 M $NaNO_3$ solution which is not observed in untreated zeolite Linde 4A (Figure 4A). As Ag^+ ions are replacing Na^+, new hydroxyl bands appear around 3661 and 3610 cm^{-1}. Two of them may be simultaneously present, depending on the Ag^+/Na^+ ratio. The frequency ratio of the hydroxyl to deuteroxyl bands is constant throughout and has the same value as found for the bending band ν_2 in Table IIA. An unambiguous assignment of the various hydroxyl frequencies is difficult. The observation that they vary in a distinct way with the degree of cation exchange suggests that the OH groups must be partially associated with or at least be influenced by the cations. Steinberg et al.[47] have given several propositions to classify the OH groups derived from their IR results with variously exchanged zeolites Y. At the present time we do not attempt to give a similar classification for the zeolite A system; we rather understand the data in Table IV as a qualitative characterization of the zeolite in its initial state, to be compared with new hydroxyl bands created during chemical reduction of the Ag^+ ions.

An additional band which disappears on deuteration is found at 758 cm^{-1}. Systematic studies are being performed in our laboratory to decide whether this band could arise from the SiOH bending vibration.

After the water signature in the unreduced zeolite is established, the discussion on the spectral changes upon chemical reduction with H_2 or D_2 can be continued.

The samples were partially dehydrated at room temperature and then exposed to 200 Torr of H_2 or D_2 at 25 °C or at 100 °C for different time intervals. Before the spectra were run, the samples were evacuated and cooled down to room temperature. Parts A and B of Figure 9 show typical spectra obtained before and after reduction with H_2 and D_2, respectively. Let us first state that the formation of HDO and D_2O, as shown in Figure 9B, constitutes a sensitive proof for the oxidation of D_2 in the silver zeolite. The reduction of the silver zeolite is accompanied by an overall decrease of transmittance and the formation of new OH and OD stretching bands listed in Table VA. These bands are already produced at low reduction degree, e.g., after reduction for 2.5 h at 25 °C with 200 Torr of D_2 (Figure 9B, curve 2). By further reduction of this sample for 20 min with D_2 at 100 °C and evacuation before cooling down to 25 °C the spectrum B3 was obtained. This procedure results in a more thoroughly dehydrated sample, in which the frequencies of the OH and OD stretching vibrations are shifted from 3621 and 2670 cm^{-1}, respectively, by about two to four wavenumbers to lower energy. After exposure of B3 to 23 Torr of water vapor followed by 1-h evacuation, spectrum B4 was obtained which shows an additional decrease of overall transmittance while the OH stretching vibrations are found at the same frequency as in B2. Spectrum B4 is almost identical with the spectrum A2. Curve A2 was obtained after 13 min reduction with 200 Torr of H_2 at 100 °C, cooling down to 25 °C, and evacuation.

(46) Bertsch, L.; Habgood, H. W. *J. Phys. Chem.* **1963**, *67*, 1621.

(47) Steinberg, K. H.; Bremer, H.; Hofmann, F.; Minachev, Ch. M.; Dimitriev, R. V.; Detjuk, A. N. *Z. Anorg. Allg. Chem.* **1974**, *404*, 129, 142. Steinberg, K. H.; Bremer, H.; Hofmann, F. *Z. Anorg. Allg. Chem.* **1974**, *407*, 162.

TABLE IV: Structural OH and OD Groups in Unreduced Silver A Zeolites, Evacuated at 25 °C[a]

	O-H			O-D			ν_{OH}/ν_{OD}		
Linde 4A									
Na_{12}-A[b]	3713			2738			1.356		
$Ag_{0.9}Na_{11.1}$-A	3713	3662		2738	2700		1.356	1.356	
$Ag_{4.3}Na_{7.7}$-A		3661			2700			1.356	
$Ag_{7.5}Na_{4.5}$-A		3660	3609		2699			1.356	
$Ag_{11.8}Na_{0.2}$-A			3610			2664			1.355

[a] Frequencies are in cm^{-1}. [b] Washed in a 0.26 M $NaNO_3$ solution.

TABLE V: Bands Formed during Reduction with H_2 and D_2

A[a]

	O-D	O-H	ν_{OH}/ν_{OD}
$Ag_{4.3}Na_{7.7}$-A	2670	3621	1.356
$Ag_{7.5}Na_{4.5}$-A	2680, 2660	3610	1.356
$Ag_{11.8}Na_{0.2}$-A	2680	3640	1.358

B[b]

	H_2 reduction		D_2 reduction
$Ag_{4.3}Na_{7.7}$-A	843	744	860
$Ag_{7.5}Na_{4.5}$-A	842	745	861
$Ag_{11.8}Na_{0.2}$-A	836	746	860

[a] Structural OH, OD groups formed in silver A zeolites upon reduction in 200 Torr of H_2 and D_2, respectively, for 10–20 min at 100 °C, followed by evacuation at 25 °C. Frequencies are in cm^{-1}. [b] Characteristic bands between 730 and 900 cm^{-1} appearing in silver A zeolites upon reduction at 100 °C in 200 Torr of H_2 or D_2 for 10–20 min, followed by evacuation and cooling to 25 °C. These bands are not present in the unreduced samples.

Interestingly, in partially reduced silver zeolite A we have discovered a high-frequency hydroxyl and deuteroxyl absorption (not shown in the figures), which appears after addition of 200 Torr of H_2, 200 Torr of D_2, 100 Torr of CO, or 15 Torr of CO_2 at 25 °C. After renewed evacuation, this band, which has never been observed in the unreduced zeolites, disappears. The width of the band is about 10 cm^{-1}. The frequency ratios for the hydroxyl to the deuteroxyl bands are exactly the same as in case of the OH, OD stretching vibrations reported in Tables IV and V. The values observed with $Ag_{4.3}Na_{7.7}$-A are ν_{OH} = 3684 cm^{-1}, ν_{OD} = 2712 cm^{-1}, ν_{OH}/ν_{OD} = 1.358; with $Ag_{7.5}Na_{4.5}$-A they are found to be ν_{OH} = 3684 cm^{-1}, ν_{OD} = 2713 cm^{-1}, ν_{OH}/ν_{OD} = 1.358. Similar values have been found with $Ag_{0.9}Na_{11.1}$-A and $Ag_{11.8}Na_{0.2}$-A.

Changes in the Range 600–900 cm^{-1}. In the spectral window between 600 and 900 cm^{-1} significant changes upon reduction can be observed. The absorption at about 758 cm^{-1} which is present in all partially dehydrated zeolites Ag_xNa_{12-x}-A and which disappears by exchanging the water with D_2O has already been mentioned. Upon reduction with H_2 and D_2 this band also vanishes. Bands generated during reduction are listed in Table VB. Further investigation is required to generate a consistent assignment of these bands.

5. Interaction of CO with Silver Zeolite A

A number of investigations on CO interaction with zeolites have appeared in the literature. Förster and co-workers have measured IR fundamental and overtone bands in NaCa-A zeolites.[23] Infrared studies of CO adsorption on different metal-exchanged zeolites have been published by several authors.[29,34,48,49] Angell and Schaffer pointed out that in dehydrated metal-exchanged zeolites X and Y adsorbed CO can be displaced by small amounts of water.[50] From this they concluded that the first sorbed water is adsorbed to the metal cations. Huang found that CO is strongly adsorbed by Ag-X and Ag-Y zeolites to the extent of four molecules per supercage at 25 °C.[51] This observation has been

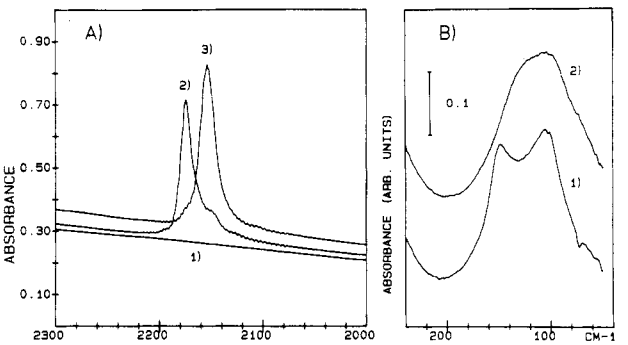

Figure 10. CO adsorption at 25 °C for different interaction times. (A) $Ag_{4.3}Na_{7.7}$-A: (1) vacuum dehydration at 150 °C; (2) 25-min exposure of (1) to 100 Torr of CO at 25 °C; (3) 4-h exposure of (1) to 100 Torr of CO at 25 °C. (B) $Ag_{11.8}Na_{0.2}$-A: (1) vacuum dehydration at 25 °C; (2) 2-h exposure of (1) to 100 Torr of CO at 25 °C.

used to determine the number of Ag^+ ions in the sodalite cage. In an elegant experiment on a silver zeolite Y it was shown that CO can be used as a label together with OH and OD stretching vibrations to follow the reduction and the oxidation of silver zeolites.[5] We extended these experiments to silver zeolite A to search for additional information in the far-IR region. According to literature at least two forms of adsorbed CO molecules should be expected. One is dominating under CO pressure; the other form remains in the zeolite even after prolonged evacuation at room temperature. Adsorbed carbon monoxide shows an increase in its stretching vibration frequency relative to the gas phase. This increase can be attributed to the stabilization of the CO bond caused by the donation of σ^*(CO) electron density to the Ag^+ in the Ag^+-(CO) complex. The samples were partially dehydrated by evacuation at room temperature or at 150 °C for 1 h. To measure the data reported in Figure 10A and Table VI [A, 1 and 2; B, 4] the thus pretreated samples were exposed to 100 Torr of CO for 10–30 min and 2–4 h. These spectra were obtained with the CO remaining in the reaction chamber. For this reason the bands A2 and A3 show some fine structure due to not fully compensated gaseous CO absorptions in the 20-cm path of our cell. The adsorption of CO obeys interesting kinetics. Slow- and fast-adsorbing species can be distinguished. Figure 10A demonstrates this for the $Ag_{4.3}Na_{7.7}$-A sample. Curve 1 was measured prior to the addition of CO, while curve 2 was recorded after 25 min reaction time with CO at room temperature. The intense band at 2174 cm^{-1} can be attributed to the CO stretching vibration of the fast-adsorbing species. After prolonged reaction time the shoulder at 2152 cm^{-1} develops to an intense single absorption at 2153 cm^{-1}, shown in spectrum 3, which has been measured after 4 h of exposure to CO, and belongs to the slowly adsorbing species. This is proved by exposing the sample to evacuation. After 1 h of evacuation the 2153-cm^{-1} band has become a shoulder again as depicted in spectrum 1 of Figure 11B. The strong absorption has nearly the same position as before, namely 2176 cm^{-1}. It is striking that the shape of this spectrum is similar to the spectrum 2 in Figure 10A, obtained after a short exposure time.

The kinetics of the CO sorption depends on the degree of silver exchange becoming faster with increasing silver content. The

(48) Huang, Y. Y. *J. Am. Chem. Soc.* **1973**, *95*, 6636.
(49) Böse, H.; Förster, H.; Frede, W.; Schumann, M. *Proc. 6th Congr. Zeolites, Reno, 1983*; **1983**, 201.
(50) Angell, C. L.; Schaffer, P. C. *J. Phys. Chem.* **1966**, *70*, 1413.
(51) Huang, Y. Y. *J. Catal.* **1974**, *32*, 482.
(52) Huber, K. P.; Herzberg, G. *Constants of Diatomic Molecules*; Van Nostrand Reinhold: London, 1979.

TABLE VI: Frequencies (cm^{-1}) of the Stretching Vibration of Carbon Monoxide Adsorbed on Silver A Zeolites[a]

	A[b]						B[c]			
	1		2	3			4	5		
Linde 4A										
$Ag_{0.9}Na_{11.1}$–A	2172	2151 (sh)	2155	2194 (w)	2171	2151 (sh)	d		2170	
$Ag_{4.3}Na_{7.7}$–A	2174	2152 (sh)	2153	2196 (w)	2176	2153 (sh)	2152	2181	2169	2154
$Ag_{7.5}Na_{4.5}$–A	2175	2151	2151	2197 (w)	2177	2154 (sh)				
$Ag_{11.8}Na_{0.2}$–A	2176 (sh)	2151	2150	2199 (w)	2182	2156 (sh)	2153	2188	2168 (sh)	2157

[a] Frequency error: about 1 cm^{-1}, for (sh) and (w) about 2–3 cm^{-1}. Gas-phase vibrations: ν_{CO} 2143.271 cm^{-1}, ν_{CO^+} 2184.68 cm^{-1}.[52] [b] A: Unreduced samples. Evacuated at 150 °C and cooled to 25 °C. (1) and (2) have been measured in presence of 100 Torr of CO atmosphere. (1) CO adsorbed after 20 min of exposure to CO. (2) CO adsorbed after 3 h of exposure to CO. (3) Adsorbed CO, remaining after evacuation of (2) for 1 h at 25 °C. [c] B: Reduced samples. Reduction for 12 h in 200 Torr of H_2 at 25 °C, followed by evacuation, and CO loading for column 4 the same as in Table VIA, column 2, and column 5 the same as in Table VIA, column 3. [d] Very weak, broad band.

amount of adsorbed carbon monoxide increases with higher silver content. Zeolite Na_{12}–A (Linde 4A) does not interact with carbon monoxide under our experimental conditions. These results are consistent with the finding of Förster and co-workers,[49] who observed (sodium zeolite)–(CO) interactions only at low temperatures.

The characteristic shape of the far-IR absorption of the fully exchanged silver zeolite A reported in Figure 6 as curve 5 and in Figure 10B as curve 1 accentuates this sample for studying the influence of CO adsorption in the far-IR region. After the zeolite $Ag_{11.8}Na_{0.2}$–A was reacted with 200 Torr of CO for 2 h, the two bands at 148 and 104 cm^{-1} merged into one band with a center of gravity at 110 cm^{-1}. It seems to have two components which, however, could not be resolved in our experiments. The band system is reversible on removing CO by evacuation. We conclude that the new band at 110 cm^{-1} is partly due to carbon monoxide physisorbed to silver cations and one may ask whether this can be understood as a Ag^+–(CO) vibration.

From the experiments of Uytterhoeven and co-workers[5] it is known that reduced silver–Y zeolites do not form chemical bonds with CO. This observation is not surprising because the donation of σ^*(CO) electron density to Ag^+, which is responsible for the formation of the Ag^+–(CO) complex, is impossible for reduced silver atoms. In order to find out what happens in the case of silver zeolite A, we reduced some of our samples in an atmosphere of 200 Torr of H_2 at room temperature in two steps: first for 2 h and then for another 10 h. The previously dehydrated samples (1 h, 150 °C) were exposed to 100 Torr of CO for 2 h at room temperature. Before the reduction was carried out, adsorbed CO was removed by evacuation for 1 h at 150 °C. After the remaining H_2 was pumped off, 100 Torr of CO was added during 2 h followed by 1 h of evacuation. The observations are collected in Table VIB and Figure 11.

First of all it is remarkable that, in the case of the unreduced samples, spectrum 1 of Figure 11, the CO absorption bands have the same shape for all silver zeolites A, differing only in frequency and intensity.

After reduction with H_2, the samples lose their capacity for CO adsorption, depending on the reduction degree. $Ag_{0.9}Na_{11.1}$–A lost nearly the whole sorption capacity after 2 h of reduction, spectrum 2 of Figure 11A. We therefore assume that it was almost completely reduced; the next reduction step shows no significant change [spectrum 3]. The first reduction step caused the important decrease of sorption capability in case of $Ag_{4.3}Na_{7.7}$–A as well [spectrum 2 of Figure 11B]. Three weak absorptions at 2181, 2169, and 2154 cm^{-1} (Table VIB) were observed after the next step, two of them being already present in spectrum 2. When the samples were heated to 150 °C under vacuum for 1 h, all bands disappeared.

The zeolite $Ag_{11.8}Na_{0.2}$–A is the only case investigated that did not lose all sorption capability by prolonged room temperature reduction with hydrogen. Its spectrum significantly changed after the first reduction step, resulting in two maxima at 2187 and 2157 cm^{-1} and a shoulder at 2171 cm^{-1}, spectrum 2 of Figure 11C. This signature becomes more pronounced after the reduction proceeds further. In this state the zeolite has a black color. Fully reduced samples can be obtained by reduction with H_2 at 100 °C. The thus-prepared wafers lost all transmittance in the visible region and in the IR region while they still show some transmittance in the far-IR.

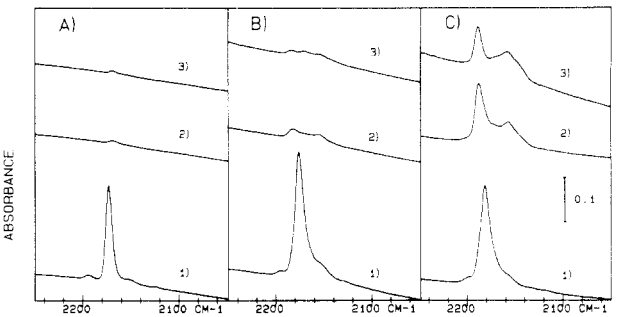

Figure 11. CO adsorption at 25 °C on silver zeolite A of different reduction degrees. Reduction was carried out at 25 °C with 200 Torr of H_2. After the remaining H_2 was pumped off, 100 Torr of CO was added over 2 h followed by 1 h of evacuation. (1) Unreduced. (2) Reduction time 2 h. (3) Total reduction time 12 h. The composition of the three samples was as follows: (A) $Ag_{0.9}Na_{11.1}$A, (B) $Ag_{4.3}Na_{7.7}$–A, (C) $Ag_{11.8}Na_{0.2}$–A.

Interestingly enough, in all cases it is possible to distinguish between chemisorbed species, having fast sorption kinetics, and physisorbed molecules. From the data reported in Table VIB it follows that the absorption maxima of the chemisorbed CO slightly shifted from 2181 to 2188 cm^{-1} while the physisorbed CO is found at nearly the same position as in Table VIA, namely at 2152–2153 cm^{-1}.

6. Interaction of CO_2 with Silver Zeolite A

Carbon dioxide on alkali-metal and alkaline-earth-metal cation-exchanged zeolites A, X, and Y leads to both physisorbed and chemisorbed species at room temperature,[53-59] different from carbon monoxide which does not interact with sodium zeolite Na_{12}–A. The asymmetric stretching vibration of physisorbed carbon dioxide on Na–A zeolites has been observed at about 2360 cm^{-1}.[56] Absorption bands in the 1800–1200-cm^{-1} region on Na–X, Na–Y, and NaCa–A zeolites are ascribed to nonlinear CO_2 species.[53,54] Several structural propositions have been given for this chemisorbed "carbonate-like" carbon dioxide.

To obtain information on the interaction of CO_2 with Ag^+ and Ag^0 in zeolitic environment we have extended CO_2 absorption studies to pure Ag^+, mixed Ag^+/Na^+, and reduced silver zeolites A. Figure 12 presents an overview of the spectrum of an $Ag_{4.3}Na_{7.7}$–A zeolite in the 4000–400-cm^{-1} region. Curve I was

(53) Jacobs, P. A.; van Cauwelaert, F. H.; Vansant, E. F. *J. Chem. Soc., Faraday Trans. 1* **1973**, *69*, 2130.
(54) Coughlan, B.; Kilmartin, S. *J. Chem. Soc., Faraday Trans. 1* **1975**, *71*, 1818.
(55) Masuda, T.; Tsutsumi, K.; Takahashi, H. *J. Colloid Interface Sci.* **1980**, *77*, 232.
(56) Delaval, Y.; Cohen de Lara, E. *J. Chem. Soc., Faraday Trans. 1* **1981**, *77*, 869.
(57) Shiralkar, V. P.; Kulkarni, S. B. *Zeolites* **1984**, *4*, 329.
(58) Delaval, Y.; Seloudoux, R.; Cohen de Lara, E. *J. Chem. Soc., Faraday Trans. 1* **1986**, *82*, 365.
(59) Förster, H.; Schuldt, M.; Seelemann, R. *Z. Phys. Chem. NF* **1975**, *97*, 329.

TABLE VII: Sorption of CO_2 on Several Silver A Zeolites[a]

	physisorbed $^{12}CO_2$				weakly bound CO_2			chemisorbed CO_2				
	$\nu_3 + \nu_1$	$\nu_3 + 2\nu_2$	ν_3	ν_2	ν_3							
Na_{12}–A[b]	3712		2352		2350	2343 (sh)		1742[c]	1655[c]	1589	1380	1207
$Ag_{0.9}Na_{11.1}$–A	3713	3599	2352		2350	2343 (sh)			1656[c]	1588	1381	1207
$Ag_{4.3}Na_{7.7}$–A	3713	3599	2351	656	2350	2342 (sh)					1383	
$Ag_{7.5}Na_{4.5}$–A	3709	3595	2348	656	2345	2338						
$Ag_{11.8}Na_{0.2}$–A			2338	656		2337	2328 (sh)					

[a] Frequencies are in cm^{-1}. [b] Washed in a solution of 0.26 M $NaNO_3$. [c] These values are taken from an experiment with deuterated samples to avoid interference with the H_2O bending mode.

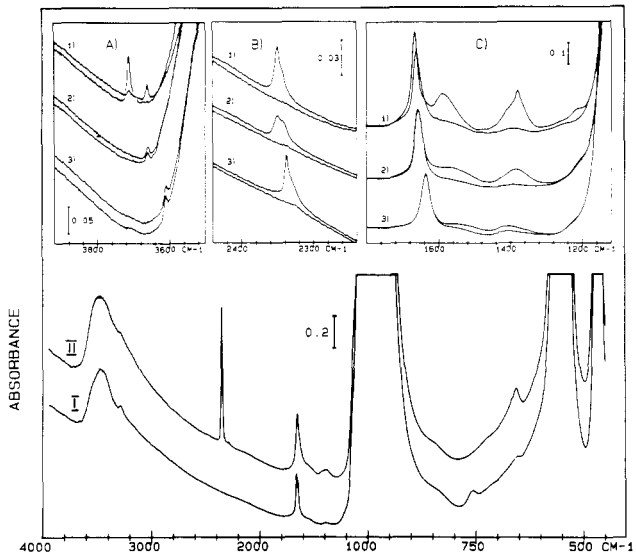

Figure 12. Adsorption of CO_2 on Ag^+ zeolites A at 25 °C. (I) and (II) are overall spectra of zeolite $Ag_{4.3}Na_{7.7}$–A. (I) Evacuated at 25 °C for 1 h (compare spectrum 1 in Figure 8). (II) Loaded for 1 h with 15 Torr of CO_2 at 25 °C and measured in CO_2 atmosphere. Absorptions of gaseous CO_2 are properly compensated. (A, B, and C) Detailed spectra of weakly bound CO_2. These spectra have been numerically scaled to a constant sample thickness of 20 μm. (1) Na_{12}–A, (2) $Ag_{4.3}Na_{7.7}$–A, (3) $Ag_{11.8}Na_{0.2}$–A. Lower trace of each pair: 1-h evacuation at 25 °C. Upper trace of each pair: 1-h adsorption of 15 Torr of CO_2 followed by 1-h evacuation at 25 °C.

obtained before adding CO_2. It is compared with the spectrum II, observed after exposing the zeolite for 1 h with CO_2 at room temperature. Specific information is obtained in the region of the hydroxyl stretching vibration at 3700 cm^{-1}. Here it is also possible to observe the $\nu_3 + \nu_1$, $\nu_3 + 2\nu_2$ combination bands of physisorbed carbon dioxide, being in Fermi resonance [see Figure 13A]. The next interesting absorptions occur in the region of the asymmetric stretching vibration ν_3 at about 2350 cm^{-1}, between 1600 and 1200 cm^{-1} where carbonate-like vibrations have been described,[53] and finally in the window between 900 and 550 cm^{-1}. This region is reversible which means that spectrum I is reproduced after 1 h of evacuation at room temperature. We therefore assign the band at 657 cm^{-1} to the bending vibration ν_2 of physisorbed CO_2 in accordance with ref 34. The shoulder at 668 cm^{-1} belongs to the Q branch of not fully compensated gaseous CO_2. There is more interesting information hidden in this spectral region which calls for detailed investigations. To complete the information, the pictures A, B, and C in the upper part of this figure show the remaining carbon dioxide absorption after 1 h of dynamic evacuation: (1) Na_{12}–A (Linde 4A washed in an aqueous 0.26 M $NaNO_3$ solution), (2) $Ag_{4.3}Na_{7.7}$–A, (3) $Ag_{11.8}Na_{0.2}$–A. The lower curve of each pair in these spectra was obtained after 1 h of evacuation at room temperature of unreacted zeolite. The upper curve of each pair was obtained after 1-h adsorption of 15 Torr of CO_2, followed by 1-h evacuation. In the case of CO_2 chemisorption on Na_{12}–A, it is interesting to note that a redistribution of structural hydroxyl groups occurs and remains stable even after prolonged evacuation; curve 1, Figure 12A. The initially strong band at 3713 cm^{-1} is reduced in favor of a new band at 3662 cm^{-1} A comparison between curves 1 and 2 shows that this new absorption is at the same position as the OH stretching vibration of partially Ag^+ exchanged zeolite A. Therefore chemisorption of CO_2 on Na_{12}–A seems to have the same effect on the distribution of structural OH groups as has the replacement of the first few Na^+ by Ag^+. In fully Ag^+ exchanged zeolite A, however, the OH band has moved to 3610 cm^{-1}, curve 3. Note that in both the fully and the partly exchanged zeolite A, the OH frequencies are unaltered on exposure to CO_2. As already mentioned, the asymmetric stretching vibration ν_3 of CO_2 on Na_{12}–A has been analyzed. It was found that this band is composed of three subbands which depend on the temperature and on the degree of hydration.[56] From Figure 12B, spectra 1, 2, and 3, it follows that with increasing silver content, the ν_3 absorption of CO_2 shifts to lower wavenumbers. For both the pure Na^+ (curve 1) and the pure Ag^+ zeolite (curve 3), this absorption is made up of two components, a main peak and a low-frequency shoulder. This profile possibly reflects the heterogeneity of adsorption sites, spectrum 2 probably being a superposition of 1 and 3. In all three cases the chemisorbed CO_2 must experience an interaction of medium strength with the zeolite, weaker, however, than the carbonate-like species because it is slowly removed on prolonged evacuation. The new absorptions in the 1600–1200-cm^{-1} region, which are assigned to carbonate-like species, are shown in Figure 12C, upper traces of curves 1, 2, and 3. The frequencies are collected in Table VII.

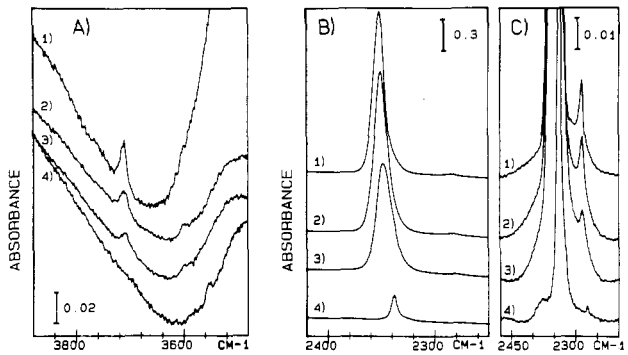

Figure 13. Physisorbed CO_2 on Ag^+ zeolites A at 25 °C. All spectra were measured in the presence of CO_2. Absorptions due to gaseous CO_2 are completely compensated. (A) Combination bands $\nu_3 + \nu_1$, $\nu_3 + 2\nu_2$. The samples were partially D_2O exchanged, evacuated overnight, and exposed to 15 Torr of CO_2 for 1 h. (B and C) ν_3 band of CO_2. (C) Shows the enlarged band of (B). The peak due to the ^{13}C isotope is very well resolved. 15 Torr of CO_2 was added for 2 h after 1-h evacuation at 25 °C. (1) Na_{12}–A, (2) $Ag_{4.3}Na_{7.7}$–A, (3) $Ag_{7.5}Na_{4.5}$–A, (4) $Ag_{11.8}Na_{0.2}$–A.

Figure 13A shows the above-mentioned combination bands of physisorbed CO_2; see also Table VII. The spectra were taken after partial exchange of H_2O with D_2O to reduce the superposition of structural hydroxyl and carbon dioxide bands. The measurement was performed with 15 Torr of CO_2. Except in the case of the fully silver exchanged zeolite A there is a clearly resolved band at about 3713 cm^{-1} and a weak one at 3600 cm^{-1}. Sample 1 contains more H_2O than the other samples; therefore the peak at 3600 cm^{-1} is less pronounced. In the fully exchanged zeolite a new band appears at 3550 cm^{-1}, whose interpretation is not yet clear. Figure 13B,C shows the ν_3 stretching bands of physisorbed $^{12}CO_2$ and $^{13}CO_2$ isotopes in their natural abundance. For $^{12}CO_2$ the band appears around 2350 cm^{-1}; it decreases in intensity and

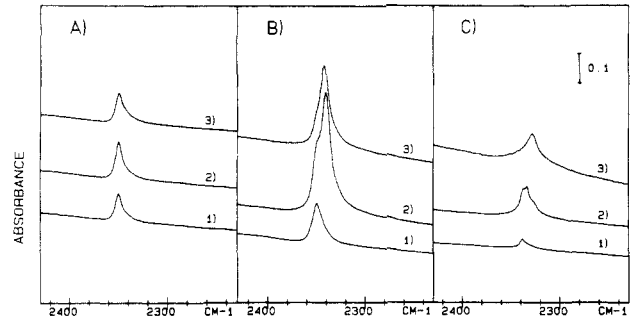

Figure 14. CO_2 adsorption at 25 °C on silver zeolite A of different reduction degrees performed with the same samples and the same conditions as described in Figure 11. After the remaining CO was pumped off at 150 °C for 1 h 15 Torr CO_2 was added over 2 h followed by 1 h of evacuation. (1) Unreduced. (2) Reduction time 2 h. (3) Total reduction time 12 h. The composition of the three samples was as follows: (A) $Ag_{0.9}Na_{11.1}$-A, (B) $Ag_{4.3}Na_{7.7}$-A, (C) $Ag_{11.8}Na_{0.2}$-A.

is bathochromically shifted for the silver-exchanged zeolites. The frequency ratio is constant for all samples and has the same value as in the gas phase (zeolite, 1.029;[35] gas peak, 1.0287[60]).

We are now interested in finding out what happens in partly reduced silver zeolites with the stretching vibration ν_3 of the weakly bound CO_2. We therefore exposed the same samples as already described in section 5 to 15 Torr of CO_2 for 1 h: (A) $Ag_{0.9}Na_{11.1}$-A, (B) $Ag_{4.3}Na_{7.7}$-A, (C) $Ag_{11.8}Na_{0.2}$-A. Before doing so the adsorbed CO was removed by evacuation at 150 °C for 1 h. The thus observed ν_3 bands after pumping off the CO_2 by 1 h of evacuation at room temperature are shown in Figure 14. We refer these bands to weakly bound CO_2 because after 1 h of evacuation at 150 °C they are completely removed.

Curve 1 represents in all three cases, A, B, and C, the unreduced zeolites. Curve 2 was obtained after 2 h and curve 3 after 12 h of reduction, leading mainly to two effects on CO_2 adsorption. The adsorption capacity is enlarged, especially for medium silver exchanged zeolites B. In all cases a new bathochromically shifted band is superposed to the absorption on the unreduced silver zeolites (curves 1). This is less pronounced for the sample $Ag_{0.9}Na_{11.1}$-A.

7. Conclusions

Infrared studies on zeolites are usually limited to the required frequency range of the bands under study. Applying modern FTIR instruments, it is now feasible to cover an enormous frequency range in a single experiment, thus opening new possibilities in exploiting complex systems. Our interest in the FTIR spectroscopy of metal-loaded zeolites is to understand interactions with gaseous reactants such as H_2O, D_2O, CO, CO_2, H_2, and D_2. For this purpose we have constructed a high-vacuum cell for in situ transmission studies on self-supporting zeolite wafers of 15-20 μm thickness and attached it to a BOMEM DA3 FTIR instrument. The experimental results reported demonstrate that very high quality information is obtained in the spectral range investigated, namely 20-13 800 cm^{-1}. We have been able to observe several new features such as Evans holes in the H_2O, D_2O stretching vibration region, overtone bands of H_2O, D_2O, and CO_2, sharp hydroxyl bands not reported up to now on zeolites A, changes in the far-IR region in presence of CO and upon reduction with H_2. It was possible to distinguish between physisorbed, weakly bound, and strongly bound (chemisorbed) carbon dioxide as well as between slowly and fast adsorbing carbon monoxide. Specific spectroscopic and kinetic investigations on the thermal and the photochemical reactivity of gaseous molecules with metal-loaded zeolites and other substrates[61] have now become more feasible.

Acknowledgment. This work was supported by Grant No. 2.025-0.86 from the Swiss National Science Foundation and Grant NEFF 329 financed by the Schweizerisch Nationaler Energieforschungsfonds. We would like to thank H. Bürgy for his contributions.

Registry No. H_2O, 7732-18-5; D_2O, 7789-20-0; H_2, 1333-74-0; D_2, 7782-39-0; CO, 630-08-0; CO_2, 124-38-9.

(60) Rothman, L. S.; Young, L. D. G. *J. Quant. Spectrosc. Radiat. Transfer* **1981**, *25*, 505.

(61) Reller, A. *Chimia* **1988**, *42*, 87.

Picosecond Dynamics of Solvent Trapping following Electron Transfer in Transition-Metal Complexes

T. Yabe, D. R. Anderson, L. K. Orman, Y. J. Chang, and J. B. Hopkins*

Department of Chemistry, Louisiana State University, Baton Rouge, Louisiana 70803
(Received: May 16, 1988; In Final Form: October 3, 1988)

Picosecond Raman spectroscopy has been used to investigate electron transfer between ligands in the metal-to-ligand charge-transfer states of D_3 transition-metal complexes. In all of the complexes studied, dynamic solvent effects on the electron-transfer process are shown to be minimal. The interligand electron coupling is apparently not strong enough to overcome the vibrational reorganization energy. As a result, delocalization of electron density over all three ligands cannot occur. An interpretation of the mechanisms responsible for producing this result is presented based on quantum mechanical electron-transfer theory.

Introduction

Over the past 10 years there has been intense interest in the photophysics of d^6 transition-metal polypyridine complexes.[1-4] Many of these complexes exhibit strong metal-to-ligand charge-transfer (MLCT) absorptions in the 350-550-nm region of the spectrum. As such, this class of molecules has been strongly pursued for potential use in solar energy conversion utilizing the water-splitting reaction. One of the issues which has been fiercely debated concerns the fate of the electron following photoinitiated

* Author to whom correspondence should be addressed.

(1) Crosby, G. A. *J. Chem. Educ.* **1983**, *60*(10), 791.
(2) Meyer, T. J. *Pure Appl. Chem.* **1986**, *58*(9), 1193.
(3) DeArmond, M. K. *Acc. Chem. Res.* **1974**, *7*, 309.
(4) Crosby, G. A.; Highland, R. G.; Truesdell, K. A. *Coord. Chem. Rev.* **1985**, *64*, 41.

0022-3654/89/2093-2302$01.50/0 © 1989 American Chemical Society